Colloid Polym Sci (2015) 293:605–615
DOI 10.1007/s00396-014-3443-1

SHORT COMMUNICATION

Morphology and conductivity tuning of polyaniline using short-chain alcohols by heterophase polymerization

Miguel A. Corona-Rivera · Víctor M. Ovando-Medina · Hugo Martínez-Gutiérrez · Francisca E. Silva-Aguilar · Elías Pérez · Iveth D. Antonio-Carmona

Received: 17 July 2014 / Revised: 21 October 2014 / Accepted: 25 October 2014 / Published online: 7 November 2014

Abstract Conducting polyaniline (PANI) nanostructures were obtained by heterophase polymerization of aniline monomer using sodium dodecyl sulfate (SDS) as surfactant in presence of the short-chain alcohols: ethanol, propanol, butanol, pentanol, and hexanol as co-surfactants, and ammonium persulfate (APS) as oxidizing agent. The resulting polymers were analyzed by Field Emission, high resolution scanning electron microscopy (FE-HRSEM), UV/Vis, FTIR, cyclic voltammetry, and X-ray diffraction (XRD). It was observed from FE-HRSEM analysis that fiber-like particles were obtained when polymerizing without alcohol and in presence of ethanol, while very big agglomerates were obtained in presence of propanol and butanol; using pentanol as co-surfactant well-defined and spherical nanoparticles were obtained, the presence of hexanol through polymerization gives both spherical agglomerated and needle-like nanostructures. Final conversions were between 50 and 73 %, in the following order: hexanol = pentanol > butanol > thanol > propanol > without alcohol. Conductivities were in the range of 0.81 to 1.1 S/m with the higher value for that synthesized in presence of pentanol. Difference in conductivity of PANI was ascribed to formation of organic acids as a consequence of reaction between alcohols and APS, thus doping in situ PANI.

Keywords Heterophase polymerization · Polyaniline · Short-chain alcohols

M. A. Corona-Rivera · V. M. Ovando-Medina (✉) · F. E. Silva-Aguilar
Ingeniería Química, Coordinación Académica Región Altiplano (COARA)—Universidad Autónoma de San Luis Potosí, Carretera a Cedral KM 5+600, San José de las Trojes, 78700 Matehuala, SLP, México
e-mail: ovandomedina@yahoo.com.mx

H. Martínez-Gutiérrez
Centro de Nanociencias y micro y nanotecnologías, Instituto Politécnico Nacional, Luis Enrique Erro S/N, D.F., 07738 México, México

E. Pérez
Instituto de Física—Universidad Autónoma de San Luis Potosí, Av. Dr. Manuel Nava No. 6 Zona Universitaria, 78210 San Luis Potosí, S.L.P., México

I. D. Antonio-Carmona
Departamento de Botánica, Universidad Autónoma Agraria Antonio Narro, Calzada Antonio Narro 1923, Buenavista, 25315 Saltillo, Coahuila, México

Introduction

Among the semiconducting polymers, polyaniline (PANI) is one of the most studied polymers as corroborated by the number of papers published in the literature in the last years. For example, the number of papers dealing with PANI published during 2013 (from Web of Science ™) was approximately 990. PANI is attracting by its chemical and physical properties like high electrical conductivity, environmental stability, stable redox activity, and ease preparation, as well as low cost [1–5], which allow some applications in areas as electrostatic dissipation, fuel cells, batteries, anion exchanger, biochemistry, inhibition of steel corrosion, sensors, anticorrosion coatings, etc. [6]. PANI can be synthesized by oxidizing aniline either electrochemically or chemically. The latter is of particular importance because this is the most practical route for the production of conducting polymers on large scale [7].

PANI can also be doped by protonation of the polymer, mechanism by which polyaniline becomes electrically conductive. However, its conductivity is influenced by various factors including its electrochemical redox state, pH, humidity, temperature, and the type of anions in the solution during its polymerization [8]. PANI nanoparticles have been also obtained by microemulsion and emulsion polymerization [9, 10], in which surfactant and dopant molecules are the key

factors determining nanoparticles morphology and electrical conductivity. For example, Jang et al. [9] have prepared conductive spherical nanoparticles of PANI by microemulsion polymerization in the presence of octyl trimethyl ammonium bromide and dodecyl trimethyl ammonium bromide as cationic surfactants, APS as oxidizing, and HCl as dopant agent. They obtained nanoparticles with diameter around 4 nm, observing that sizes can be tuned changing the surfactant spacer length, surfactant concentration, and polymerization temperature. PANI nanoparticle revealed enhanced conductivity compared to conventional bulk PANIs. The conductivity of PANI nanoparticle increased up to 84.6 S/cm at 3 °C compared to 2.9 S/cm at 60 °C. Yan and Xue [11] have also synthesized PANI nanoparticles by reverse globular microemulsions using APS as oxidizing, sodium dodecylbenzene sulfonate (DBSA) as stabilizing, HCl as dopant agent, and butanol and hexane as continuous phase at room temperature. They obtained spherical PANI nanoparticles with diameters in the range from 30 to 60 nm with conductivity of 1.5 S/cm. Also, PANI with high crystallinity was obtained, which was ascribed to the orientation behavior of the molecularly ordered microemulsion system. Biocatalyzed synthesis of PANI has been also reported in reversed microemulsions. For example, Chen et al. [12] obtained PANI using cyclohexane as continuous phase and DBSA as surfactant and hemoglobin and H_2O_2 as biocatalyzing system. They observed that conductivity values were as high as 0.9 S/cm and needle-like nanoparticles with an average diameter of 30–50 nm and 200–800 nm in length. Gul et al. [7] have prepared PANI by reverse emulsion polymerization using a mixture of chloroform and 2-butanol as dispersing medium and DBSA as surfactant with benzoyl peroxide as oxidant. They obtained completely soluble PANI in dimethyl sulfoxide, dimethylformamide, chloroform, and in a mixture of toluene and 2-propanol; unfortunately, conductivities were not reported in that work.

In this work, we present the synthesis of PANI in the presence of different alcohols. In this synthesis, aniline was polymerized by chemical oxidation in batch heterophase mode using sodium dodecyl sulfate (SDS) as surfactant and different short-chain alcohols as co-surfactant to modulate the particle morphology and conductivity of PANI. To the best of our knowledge, there are no systematic reports about the

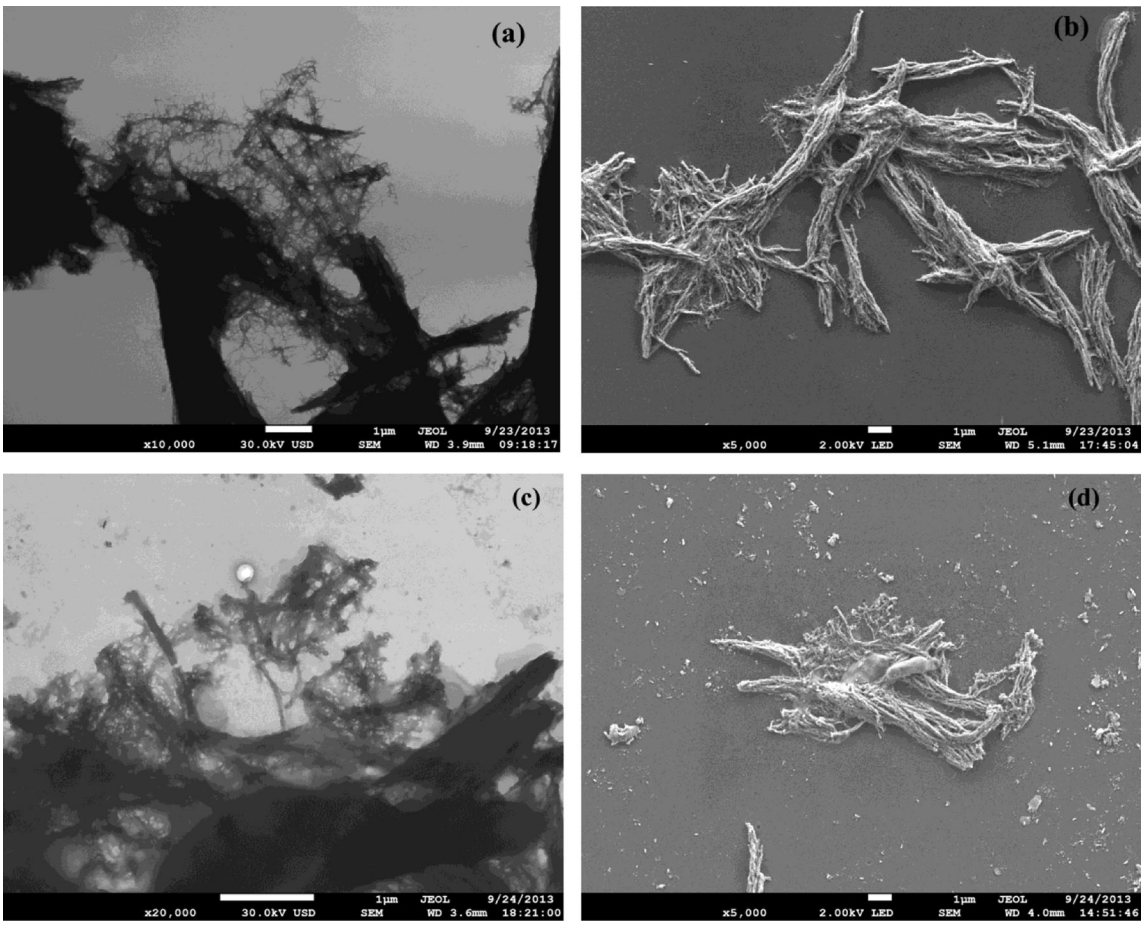

Fig. 1 Scanning electron micrographs in STEM mode (**a**) and (**c**) of PANI synthesized without alcohol and with ethanol, respectively; and the corresponding SEM image (**b**) and (**d**)

effects of different alcohol types throughout aniline polymerization on conductivity and nanostructure of the resulting PANI.

Experimental

Materials

Aniline (≥99.5 %), ethanol (≥99 %), butanol (≥99.8 %), pentanol (≥99 %), and APS (98 %) were acquired from Sigma-Aldrich (Toluca, Mexico). Propanol (99 %) and hexanol (99 %) were purchased from J.T. Baker (PA, USA). SDS was acquired from Hycel (Guadalajara, Mexico >99 %). All reactants were used as received. Distilled grade water was used in all the experiments.

Polymerizations

In a typical reaction, 17.3 mmol of SDS were dissolved in 150 g of water and stirred during 10 min. Then, 21 mmol of alcohol was added to the solution for each of the different reactions and homogenized. After that, 21 mmol of aniline was added and homogenized with magnetic stirring, obtaining a clear and translucent mixture. The mixture was bubbled with argon of ultrahigh purity (Infra ^{TM} >99.999 %) through 20 min. Twenty-one millimoles of APS was added under magnetic stirring at room temperature to start polymerization. Reaction proceeded throughout 6 h. At the onset of polymerization a brown color was observed, and a dark green solid precipitate was formed at the end of polymerizations. The reaction mixture was poured into an excess of methanol to precipitate the PANI nanoparticles and to remove impurities. The samples were decanted and dried at 60 °C in a vacuum oven during 24 h. Conversions were determined gravimetrically by repeating the polymerizations and drying the total reaction mixture and subtracting the known weights of surfactant and APS from the total weight of the dried samples.

Characterization

The resulting materials were analyzed using UV/Vis spectroscopy (GENESYS 10, Thermo-Spectronic). The samples were also analyzed by FTIR spectroscopy (PerkinElmer, Spectrum

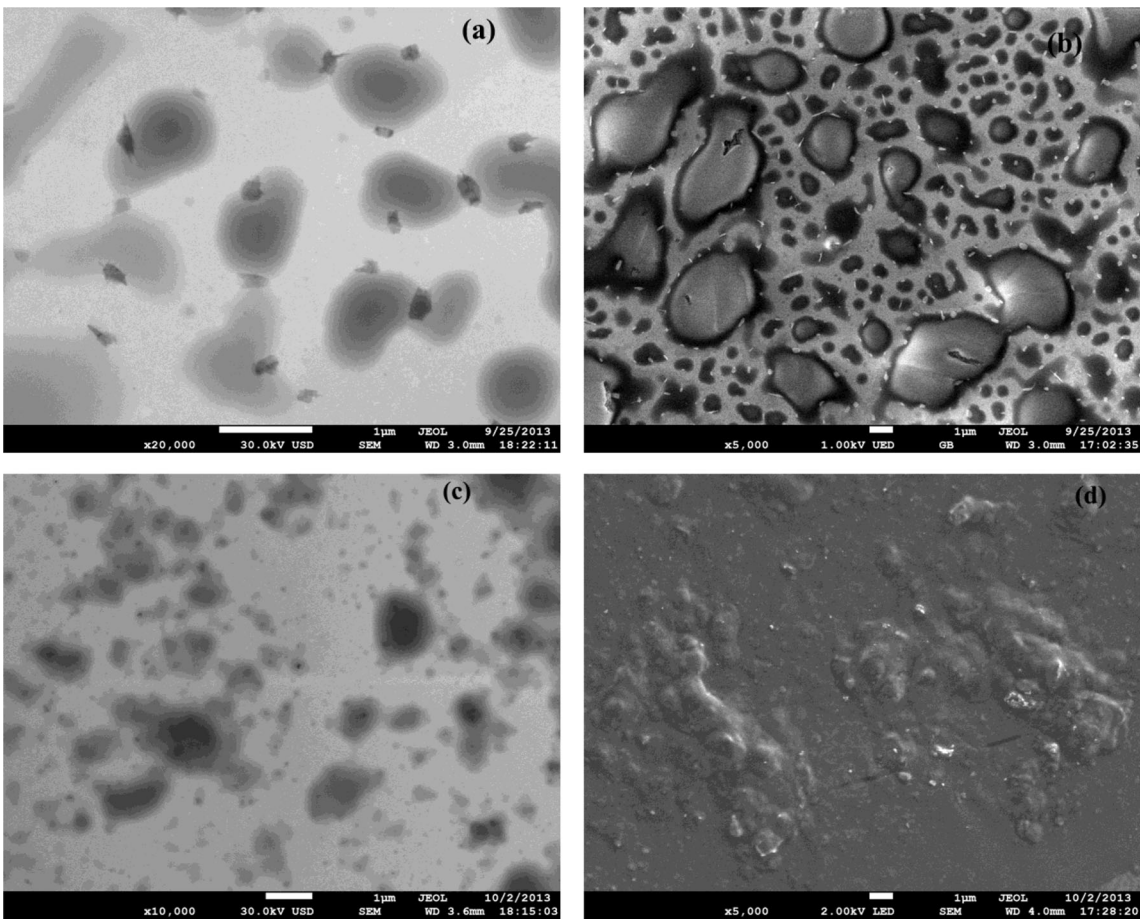

Fig. 2 Scanning electron micrographs in STEM mode (**a**) and (**c**) of PANI synthesized with propanol and with butanol, respectively; and the corresponding SEM image (**b**) and (**d**)

™ One). The redox activity of PANI was analyzed by cyclic voltammetry measurements performed in a glass cell using a potentiostat/galvanostat GAMRY (G-300). Platinum disc, platinum wire, and Ag/AgCl electrodes as the working, counter, and reference electrodes were used respectively. Voltammetry scans were carried out by dispersing 0.1 g of sample in 100 mL of aqueous solution 0.1 M H_2SO_4 at room temperature in a potential range of −0.20 to +0.80 V using a scan rate of 100 mV/s.

The X-ray diffraction (XRD) analysis was made with a Rigaku instrument (Miniflex 600, Cu K_α (λ=1.54 Å)) at 3°/min of scanning speed from 10° to 55° of 2θ. For the morphology and particle size determination and distribution, a 1:1000 water dilution of the latex without purification was used. A drop of the diluted latex was poured onto a copper grid coated with Formvar™ resin and carbon film, and then, it was allowed to dry overnight at room temperature. The samples were analyzed by scanning electron microscopy in SEM (at 2 or 1 kV of acceleration voltage with secondary electron detector) and STEM (a 30-kV acceleration voltage with a bright field transmitted electron detector) modes using a Field Emission High Resolution SEM (JEOL, JSM-7800F). The electrical conductivities of samples were determined by the four-probe method (SP4 probe head Lucas/Signatone with 0.04 in of spacing between tips) coupled to a Keithley (2400 SourceMeter) instrument.

Results and discussion

Particle morphology

Since a practical point of view, STEM mode contrast all the nonvolatile species deposited on the sample grid, including polymer, residual surfactant, and initiator salts. To avoid uncertainties in image interpretation, STEM images were complemented with SEM (topography of samples). So in Figs. 1, 2, and 3, we found that the more strong darkened areas observed in STEM images correspond to the more strong bright areas of SEM and in both cases are corresponding with polyaniline phase.

Figure 1 shows the scanning electron micrographs in STEM mode of PANI synthesized without alcohol (1a) and with ethanol (c) and the corresponding SEM image (b) and

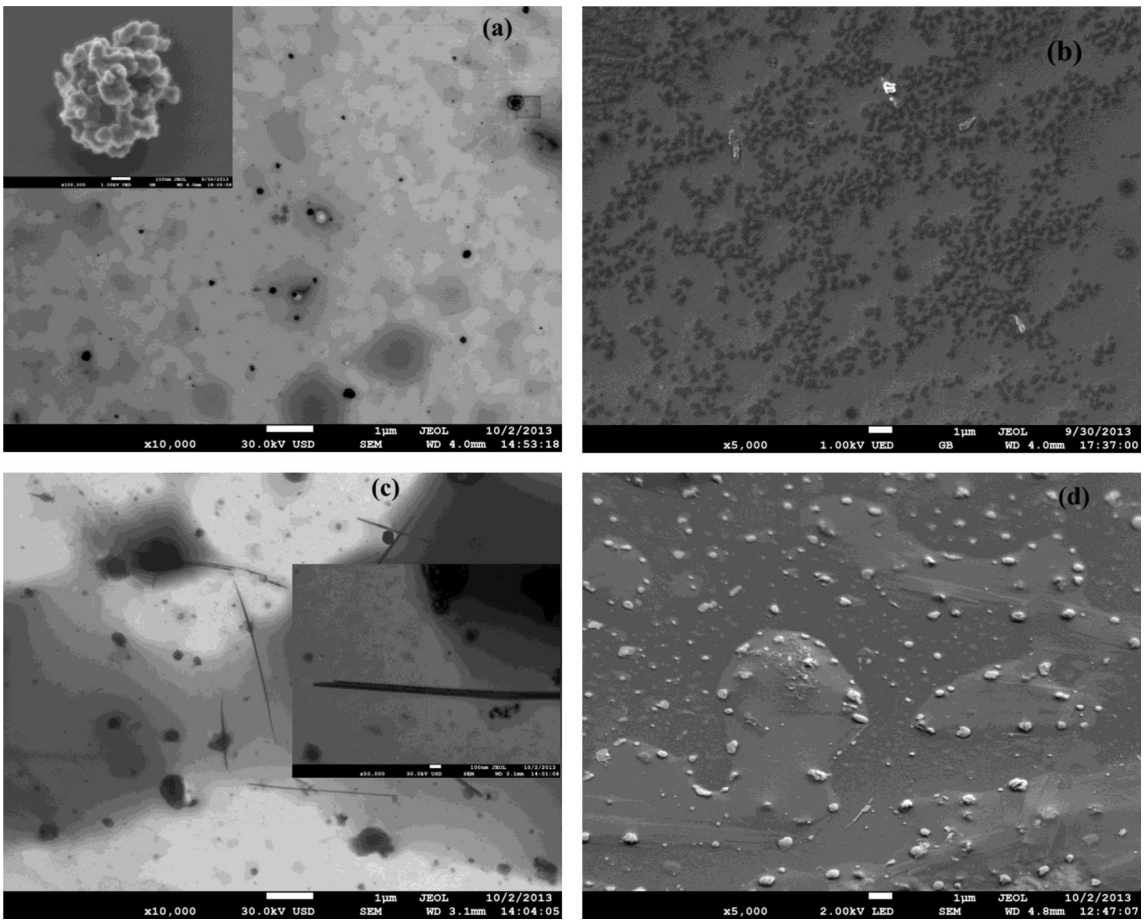

Fig. 3 Scanning electron micrographs in STEM mode (**a**) and (**c**) of PANI synthesized with pentanol and with hexanol, respectively; and the corresponding SEM image (**b**) and (**d**)

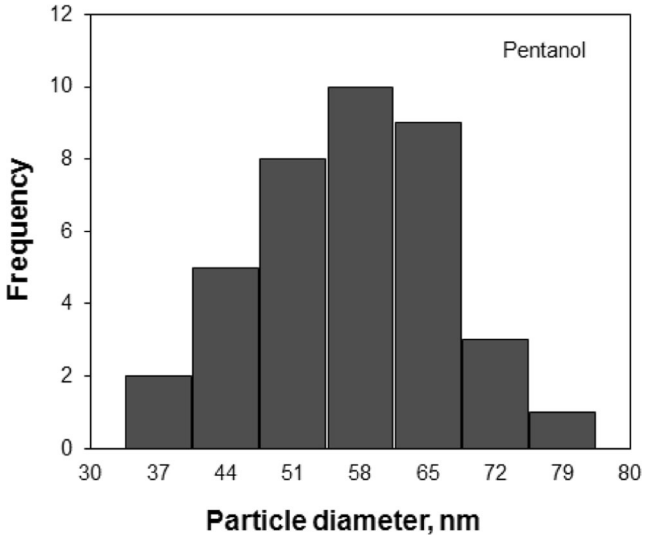

Fig. 4 Particle size distribution of spherical nanoparticles of PANI obtained polymerizing in presence of pentanol as co-surfactant

(d). It can be observed that well-defined fibrillar nanostructures were obtained in these two cases. However, nanostructures with ethanol tend to deform fibrillar morphology as a result of interaction of ethanol tail with aniline monomer through polymerization. Fibrillar morphology has been previously reported for aqueous polymerization of aniline [13, 14]. In Fig. 1, very large fibers (approx. 5 μm in large) and between 60 and 90 nm of width are observed for aniline polymerization without alcohol, while 50 and 85 nm of width were observed for polymerization in presence of ethanol. Also, some agglomerates were formed in presence of ethanol, losing some of the fibrillar morphology. Osorio et al. [13] synthesized fibrillar nanostructures of PANI co-doped and co-oxidized with a molar ratio of HCl/camphorsulfonic acid (CSA) of 0.4/0.6 and 0.2/0.8 and polymerized in aqueous solutions of aniline. They observed fibers with average diameters between 60 and 100 nm and average length between 300 and 500 nm, both decreasing with the molar ratio of HCl/CSA. Haba et al. [14] polymerized aniline in presence of DBSA as both: dopant and surfactant, observing needle-like structures at the beginning of polymerization and globular structures at intermediate times; however, agglomerates were observed at the end of polymerization.

PANI morphologies were strongly affected by increasing the alcohol tail. Figure 2 shows the scanning electron micrographs in STEM mode (a) and (c) of PANI synthesized in presence of propanol and butanol, respectively; and the corresponding SEM image (b) and (d). It can be seen that fibrillar structures were not present with very big PANI agglomerates in both cases. By increasing the alcohol chain length used through aniline polymerization from butanol to pentanol and hexanol, new defined structures were obtained, as can be observed in Fig. 3. For example, by using pentanol as co-surfactant, small agglomerates consisting of well-defined spherical nanoparticles were observed (inset in Fig. 3a at ×100,000 of magnification).

The number- and weight-average particle diameters (D_n and D_w) and polydispersity index in sizes (PDI) of the PANI nanoparticles synthesized using pentanol as co-surfactant were calculated using the following equations [15]:

$$D_n = \sum n_i D_i / \sum n_i \quad (1)$$

$$D_w = \sum n_i D_i^4 / \sum n_i D_i^3 \quad (2)$$

$$\mathrm{PDI} = D_w / D_n \quad (3)$$

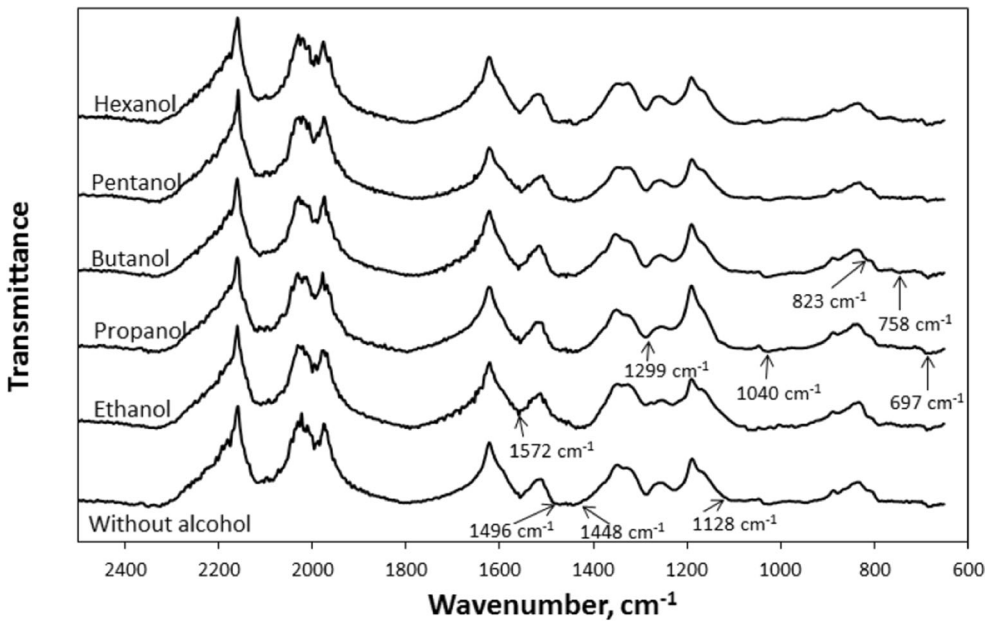

Fig. 5 Infrared spectra of PANI obtained in the different syntheses

Scheme 1 Chemical structure of PANI and its different oxidation states [8]

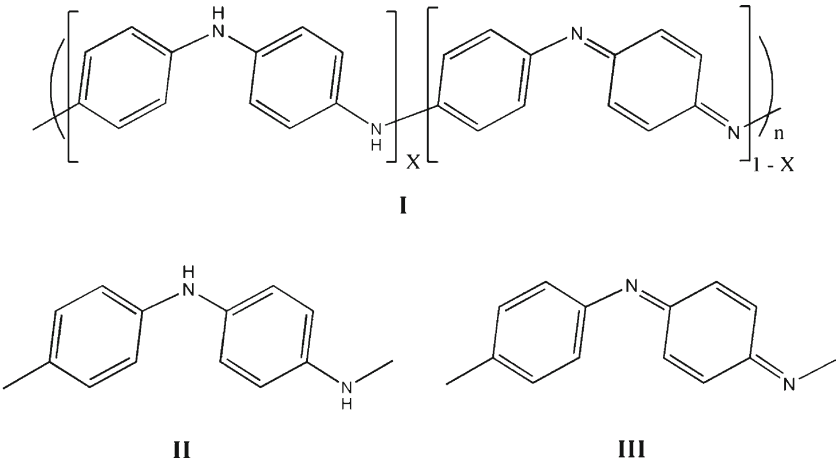

where n_i is the number of particles with diameter D_i.

The calculated values of D_n and D_w were 56 and 61 nm, thus giving a PDI of 1.1, which imply that narrow and monomodal particle size distribution can be synthesized by using pentanol, as can be seen in Fig. 4.

Changing to hexanol as co-surfactant, needle-like structures were obtained, as can be observed in Fig. 3c, with diameters between 25 and 40 nm (inset in Fig. 3c at ×50,000) and 4 μm in length. Also, spherical nanoparticles near to 50 nm of diameters were formed.

The morphology of resulting polymer nanoparticles is essentially dependent on the micelle structure derived from the surfactant assembly such as spherical, cylindrical, and layer structures. The results found here imply that different surfactant/alcohol associations are acquired before aniline polymerization by changing alcohol chain length. Anilkumar and Jayakannan [16] synthesized PANI with fiber, rod, sphere, and tube nanostructures using an amphiphilic azobenzene molecule (4-[4-hydroxy-2-((*Z*)-pentadec-8-enyl)phenylazo] benzenesulfonic acid) which acts as dopant and surfactant and changing the polymerization medium from emulsion to interfacial polymerization.

Morphologies shown here are also known as one dimension (1D) nanostructure. The fabrication of 1D polyaniline with nanometer dimensions have attracted intensive interest because they possess the advantage of both low-dimensional system and can be envisioned for applications including polymeric conducting molecular wires, chemical sensors, biosensors, and light-emitting devices [17].

Polymer composition and conductivity of PANI nanostructures

Figure 5 shows the FTIR spectra of PANI nanoparticles obtained without and with different alcohols. It can be seen the characteristic peaks of the PANI base, which are at 1572, 1496, 1448, 1299, 1128, 1040, 823, 758, and 697 cm^{-1}. The band at 1448 cm^{-1} is related to mixed C–C stretching and C–H and C–N bending vibrations observed in the spectra of the aromatic oligomers. The peak at 1040 cm^{-1} possibly corresponds to the S=O stretching vibration and suggests the presence of sulfonic groups on the aromatic rings. These groups result from persulfate radical attack to benzene rings. The bands at 758 and 697 cm^{-1} are characteristic of monosubstituted aromatic rings that are located at the ends of chains. Their observation indicates the presence of short-chain oligomers [18, 19]. Peaks at 1572 and 1128 cm^{-1} can be ascribed to C=C stretching of quinoid rings (*Q*); peak at 823 cm^{-1} is due to C–H aromatic out of plane bending of 1,4-ring. Signal at 1299 is characteristic of C–N stretching in the *Q*/cis-benzenoid (B_c)/*Q*, *Q*/benzenoid ring (*B*)/*B*, and *B*/*B*/*Q* of PANI [1]. Peak at 1496 cm^{-1} is due to PANI base, as is consistent with quinone and benzene ring stretching deformations [3].

As stated by Song et al. [8], oxidation state and doping degree are key factors determining conductivity of PANI. The three oxidation states are the fully reduced known as leucoemeraldine which contains only amine groups (**II** in Scheme 1), the fully oxidized made-up of imine groups, also known as pernigraniline (**III** in Scheme 1), and the half oxidized or emeraldine (X=0.5 of **I** in Scheme 1).

Table 1 Conductivity values of synthesized PANI and pH of latexes

Alcohol used	Conductivity (S/m)	Conversion (%)	Initial pH; final pH
Without alcohol	0.840	50	3.1; 2.1
Ethanol	0.965	63	3.3; 2.2
Propanol	0.901	61	3.2; 2.8
Butanol	0.956	67	3.4; 2.7
Pentanol	1.094	73	3.2; 2.6
Hexanol	0.808	73	3.1; 2.8

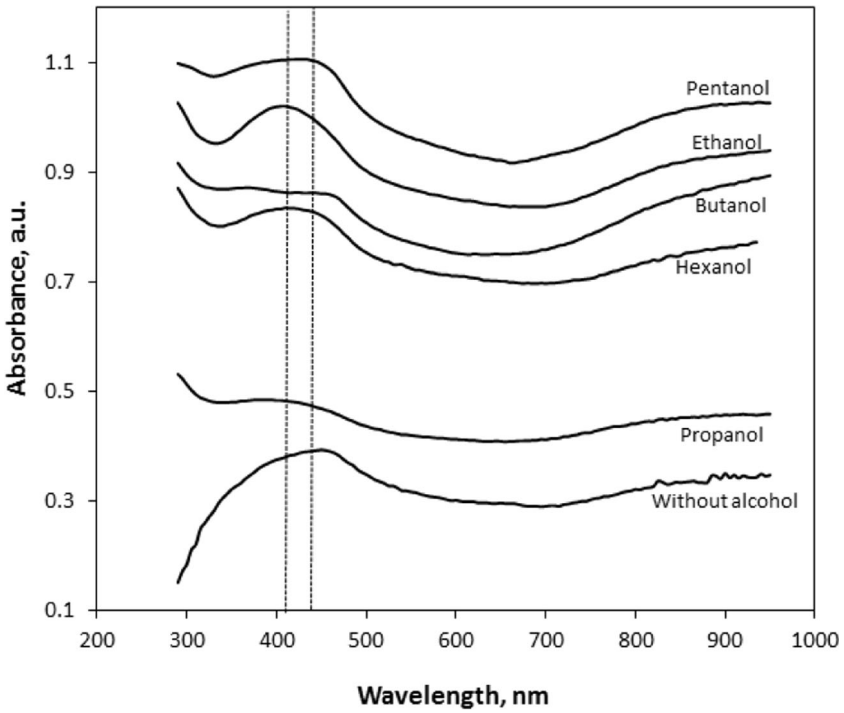

Fig. 6 UV/Vis spectra of final PANI obtained in presence of different alcohols

The chains of conducting PANI have ordered structure; they contain regularly alternating phenyl rings and nitrogen-containing groups. This structure provides for polyconjugation: polymer chain forms a zigzag lying in one plane, and π-electron clouds overlap above and below this plane. The lone electron pair of nitrogen performs the same function as π-electrons and assures polyconjugation [20]. The imine nitrogen atoms can be protonated in an acidic environment (doping process). The degree of protonation depends on the oxidation state of polyaniline and pH of the aqueous solution in which the polymer is immersed.

As shown in Table 1, conductivity of PANI increased about 15 % when using ethanol and 30 % using pentanol as co-surfactants, respectively compared to PANI synthesized without any alcohol. This behavior can be explained as a function of doping degree. In all cases, initial pH values are near to 3.2 and decreases at the end of polymerizations to values between 2.1 for that obtained without alcohol and 2.8 for that

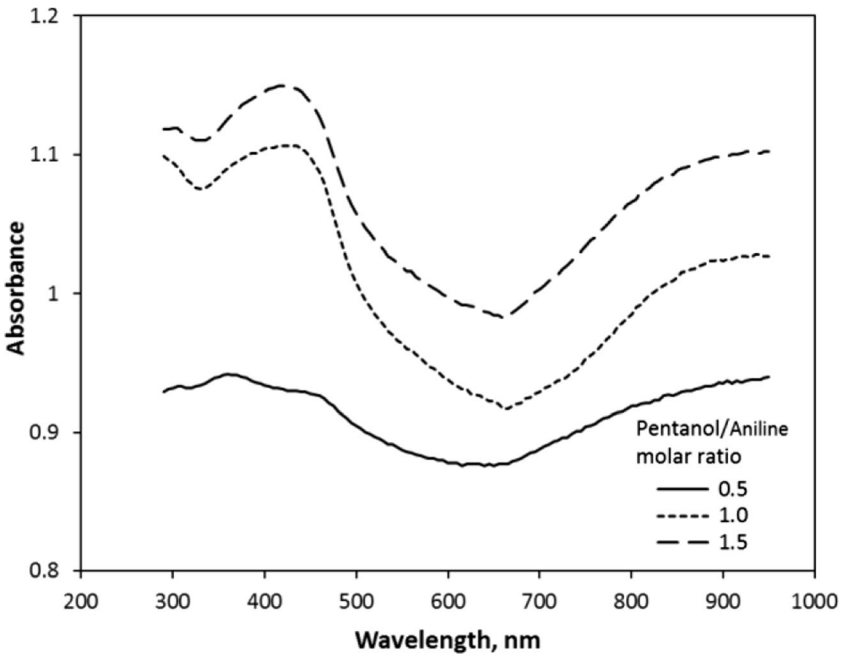

Fig. 7 UV/Vis spectra of final PANI obtained at different pentanol to aniline molar ratios

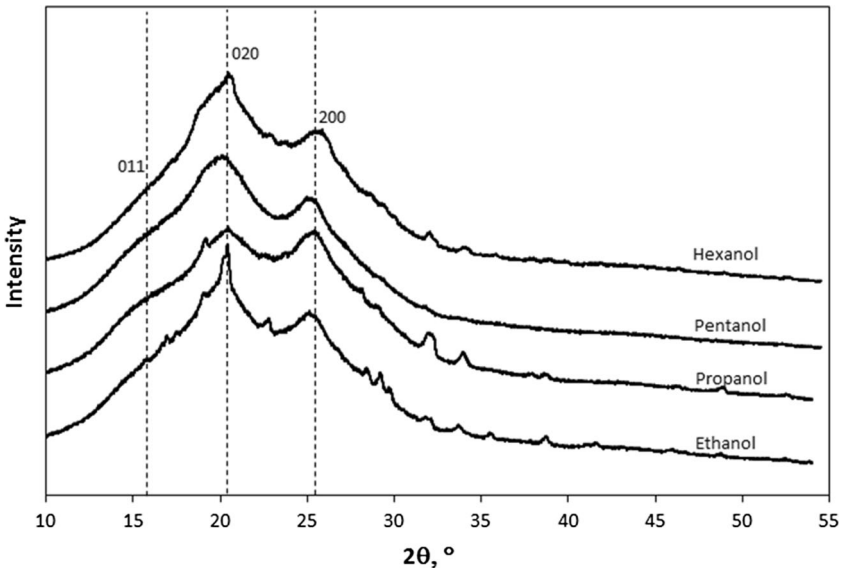

Fig. 8 XRD spectroscopy of PANI obtained in presence of different alcohols

synthesized in presence of propanol and hexanol. These results suggest that acids are produced through polymerizations. It has been reported that when PANI is synthesized in the presence of methanol, some formic acid and formaldehyde are produced as a result of the reaction between methanol and APS [21]. Thus, acids derived from reactions between alcohols and APS can be doping PANI, increasing its conductivity.

Figure 6 shows the UV/Vis spectra of PANI obtained in the different polymerizations. The absorption spectra of PANI show bands around 300 and 540 nm corresponding to π-π* transition within the benzenoid moieties and due to the formation of a doping level owing to the "exciton" transition caused by inter-band charge transfer from benzenoid to quinoid moieties, respectively. The localized polaron peak around 900 nm indicates a compact coiled conformation of PANI revealing the presence of PANI in its conducting form [22]. The maximum absorbance of the first peak for PANI synthesized without alcohol is centered at 440 nm, whereas in the

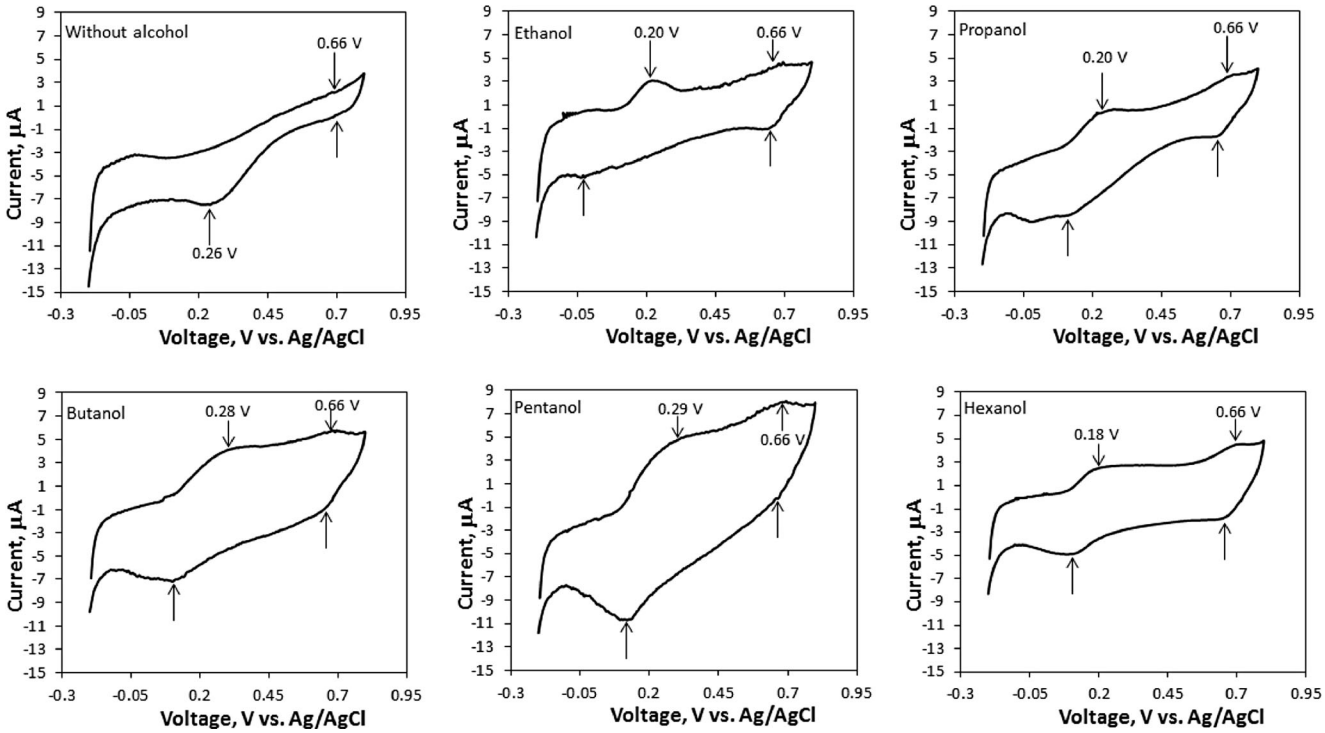

Fig. 9 Cyclic voltammetry curves of PANI obtained in presence of different alcohols

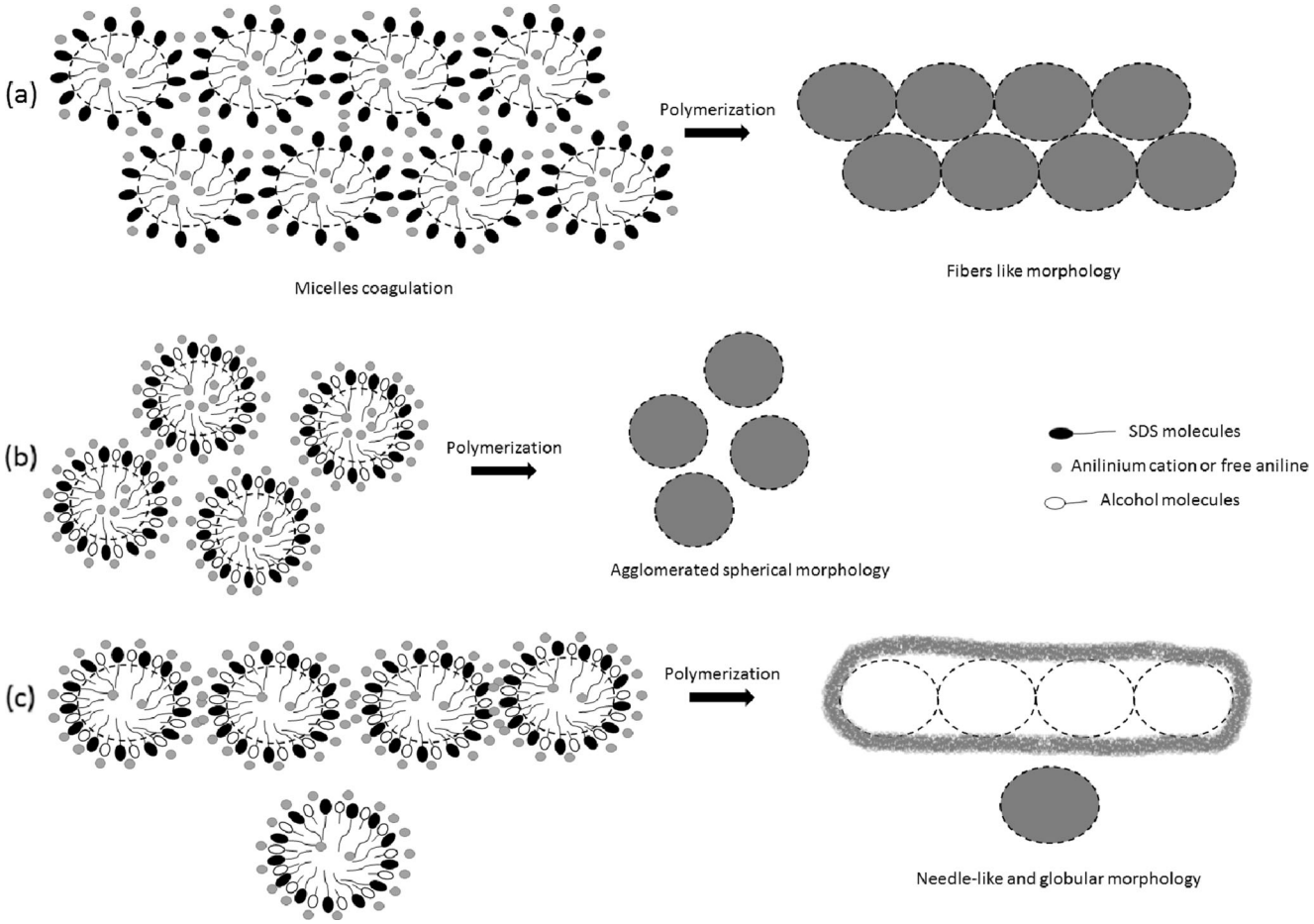

Fig. 10 Proposed mechanisms for the different nanostructures of PANI obtained changing the alcohol type

presence of alcohols, the maximum absorbance is shifted to 405 nm, except for PANI obtained in presence of pentanol, which was near to 440 nm.

In order to demonstrate the effect of pentanol on electrical properties of PANI, reactions were carried out varying pentanol concentration, and the UV/Vis spectra are shown in Fig. 7. It can be observed that intensity of band corresponding to π-π* transitions increases with pentanol amount, thus more conductive PANI can be formed, which is in agree with conductivity values 0.9, 1.1, and 1.9 S/m for molar ratios of pentanol/aniline of 0.5, 1.0, and 1.5, respectively. This behavior was also observed for propanol with PANI conductivities of 0.83, 0.90, and 0.92 S/m for the same molar ratio of alcohol/aniline. For the other alcohols used, conductivities were not strongly affected by the alcohol concentration.

Selected XRD patterns are shown in Fig. 8. It can be observed two sharp peaks at 2θ=20.5° and 25.5° showing the presence of high crystallinity and condensed structure. The peak at 20.5° can be ascribed to periodicity parallel to polymer chain [9], and the peak at 25.5° is assigned to the periodicity due to stacking of polymer chains in the perpendicular direction of chain axis [13]. These two peak along with that at 15.5° fit with the pattern of an orthorhombic structure. Crystallinity is related to conductivity of conducting polymers: the greater the crystallinity degree, the higher the conductivity; however, in our case, conductivity depends also on the oxidation state of PANI.

Electrochemical characterization

The voltammetry curves of samples from the different syntheses are shown in Fig. 9. There, we observe the characteristic curves of PANI for samples obtained in presence of alcohols; however, for sample obtained without alcohol, only one cathodic peak (almost negligible) can be observed at 0.66 V. Samples synthesized in presence of alcohols showed two cathodic and anodic peaks. First cathodic peak shifted from 0.2 to 0.28 V by changing alcohol from ethanol to pentanol; this value decreased to 0.18 V using hexanol. Sample with higher redox activity was that obtained with pentanol, which is in agreement with the results of UV/Vis and conductivity. Potentials at which cathodic peaks appear are similar to that reported by Pruneanu et al. [23]. Snauwaert et al. [24] demonstrated that the ratio of amine to imine groups of PANI is a function of electrochemical potential at 0.15 V; the protoemeraldine content is approximately 25 %, and at

0.6 V, the PANI form corresponds to approximately 50 % of emeraldine; after 0.8 V, more than 80 % corresponds to pernigraniline form. Then, in our results, the first peak is attributed to oxidation of leucoemeraldine to emeraldine form of PANI, and the peak about 0.65 V is due to the oxidation from the emeraldine to the pernigraniline state [23]. As can be seen in Fig. 9, no redox peaks were observed at intermediate potentials; thus, the presence of overoxidized units, branched polymer, or degradation of soluble species from PANI can be neglected [23, 25].

Relationship of alcohol type with morphology and conductivity

As explained by Chen et al. [26], PANI nanostructure can be modified from spherical to fiber-like depending on both: pH of polymerization medium and stabilizing agents. For example, they used mixtures of sodium dodecyl benzene sulfonic acid (SDBA) and SDS in different molar ratios. They observed that high molar ratios of SDBA to SDS produced mainly spherical structures, whereas increasing the SDS concentration results in mixed spherical and cylindrical morphology. A proposed mechanism of PANI nanostructures obtained in our work is shown in Fig. 10. When SDS is dissolved in water, globular micelles are present, because we are using a concentration of 115 mM of SDS (the critical micellar concentration of SDS is 8 mM [26]); and when alcohols were added, alcohol molecules are placed between the polar heads of SDS molecules. The main function of alcohol was to increase particle stability throughout polymerization. For low SDS concentrations, aniline molecules exist as anilinium cations in the micelle-water interface, which can be neutralized by the presence of higher SDS concentrations to produce free aniline molecules, which reside inside the micelles [26]. Then, when no alcohol was used, micelles are not spherical at all and upon polymerization particle coagulation was verified (Fig. 10, part a), polymerizing in both: inside the micelles and at the micelle-water interface forming fibers, consisting of diameters among 60 and 90 nm (Fig. 1b). For polymerizations in presence of ethanol, particles are more stable and fiber diameters decreased to values between 55 and 85 nm (Fig. 1d); by increasing the alcohol chain length, to propanol and butanol, fiber structures are not present any more, and particles consist of very big agglomerated globular structures; and when pentanol was used, particles are so stable that only globular structures are formed (Fig. 10, part b). For alcohol chain length as long as hexanol, particles become unstable again due to high separation of polar heads of SDS molecules, resulting in particle coagulation but not as unstable as polymerization without alcohol; thus, both needle-like and globular structures were observed.

As discussed before, alcohols not only react with APS producing organic acids, doping PANI, and increasing conductivity but also the nanostructures can affect PANI conductivity. Ordered globular structures obtained with pentanol can be packed in a better way than fibers or needle-like structures, thus increasing PANI crystallinity as can be seen from XRD analysis in Fig. 8, the greater the crystallinity, the higher the conductivity.

Conclusions

Conductivity and morphology of PANI were tuned by polymerizing in the presence of different short-chain alcohols. Fibrillar nanostructures were observed without alcohol and in presence of ethanol, respectively. In the presence of propanol and butanol, very large PANI agglomerates were obtained; and by increasing the alcohol chain length to pentanol, structures consisting of well-defined spherical nanoparticles between 56 and 61 nm were formed with monomodal and narrow PSD, while the presence of hexanol resulted in needle-like structures. The higher conductivity of PANI was that synthesized using pentanol (1.9 S/m for a molar ratio of pentanol to aniline of 1.5), which was ascribed to formation of acids and aldehydes derived from reactions between alcohol and APS thus doping PANI, increasing its conductivity and redox activity.

Acknowledgments V.M.O.M. wants to thank to the Consejo Nacional de Ciencia y Tecnología (CONACyT—México) by Grant No. SEP-80843. Especial thanks are given to José A. Andraca-Adame for his help in XRD analysis and to the Centro de Nanociencias y micro y nanotecnologías-IPN for the facilities in SEM characterization.

References

1. Pérez-Martínez CJ, del Castillo-Castro T, Castillo-Ortega MM, Rodríguez-Félix DE, Herrera-Franco PJ, Ovando-Medina VM (2013) Preparation of polyaniline submicro/nanostructures using l-glutamic acid: loading and releasing studies of amoxicillin. J Synth Met 184:41–47. doi:10.1016/j.synthmet.2013.09.027
2. Chen J, Winther-Jensen B, Pornputtkul Y, West K, Kane-Maquire L, Wallace GG (2006) Synthesis of chiral polyaniline films via chemical vapor phase polymerization. Electrochem Solid-State Lett 9:C9–C11. doi:10.1149/1.2136247
3. Blinova NV, Stejskal J, Trchová M, Prokes J (2008) Control of polyaniline conductivity and contact angles by partial protonation. Polym Int 57:66–69. doi:10.1002/pi.2312
4. Bhadra S, Khastgir D, Singha NK, Lee JH (2009) Progress in preparation, processing and applications of polyaniline. Prog Polym Sci 34:783–810. doi:10.1016/j.progpolymsci.2009.04.003
5. Wang YM (2014) Microwave absorbing materials based on polyaniline composites: a review. Int J Mater Res 105:3–12. doi:10.3139/146.110996
6. Xia H, Wang Q (2001) Synthesis and characterization of conductive polyaniline nanoparticles through ultrasonic assisted inverse

microemulsion polymerization. J Nanoparticle Res 3:399–409. doi:10.1023/A:1012564814745
7. Gul S, Shah AA, Bilal S (2013) Synthesis and characterization of processable polyaniline salts. J Phys Conf Ser 439(012002):1–10. doi:10.1088/1742-6596/439/1/012002
8. Song E, Choi JW (2013) Conducting polyaniline nanowire and its applications in chemiresistive sensing. Nanomaterials 3:498–523. doi:10.3390/nano3030498
9. Jang J, Ha J, Kim S (2007) Fabrication of polyaniline nanoparticles using microemulsion polymerization. Macromol Res 15:154–159. doi:10.1007/BF03218767
10. Kwon JY, Kim EY, Kim HD (2004) Preparation and properties of waterborne-polyurethane coating materials containing conductive polyaniline. Macromol Res 12:303–310. doi:10.1007/BF03218404
11. Yang F, Xue G (1999) Synthesis and characterization of electrically conducting polyaniline in water–oil microemulsion. J Mater Chem 9: 3035–3039. doi:10.1039/A905146E
12. Chen J, Bai L, Yang M, Guo H, Xu Y (2014) Biocatalyzed synthesis of conducting polyaniline in reverse microemulsions. Synth Met 187: 108–112. doi:10.1016/j.synthmet.2013.10.026
13. Osorio-Fuente JE, Gómez-Yáñez C, Hernández-Pérez MA, Corea-Téllez ML (2013) Submicrometric fibrillar structures of codoped polyaniline obtained by co-oxidation using the NaClO/ammonium peroxydisulfate system: synthesis and characterization. J Mex Chem Soc 57:306–313
14. Haba Y, Segal E, Narkis M, Titelman GI, Siegmann A (1999) Polymerization of aniline in the presence of DBSA in an aqueous dispersion. Synth Met 106:59–66. doi:10.1016/S0379-6779(99)00100-9
15. Ovando-Medina VM, Peralta RD, Mendizábal E, Martínez-Gutiérrez H, Lara-Ceniceros T, Ledezma-Rodríguez R (2011) Synthesis of polypyrrole nanoparticles by oil-in-water microemulsion polymerization with narrow size distribution. Colloid Polym Sci 289:759–765. doi:10.1007/s00396-011-2394-z
16. Anilkumar P, Jayakannan M (2008) Divergent nanostructures from identical ingredients: unique amphiphilic micelle template for polyaniline nanofibers, tubes, rods, and spheres. Macromolecules 41:7706–7715. doi:10.1021/ma801090f
17. Kumar S, Singh V, Aggarwal S, Mandal UK (2009) Synthesis of 1-dimensional polyaniline nanofibers by reverse microemulsion. Colloid Polym Sci 287:1107–1110. doi:10.1007/s00396-009-2078-0
18. Konyushenko EN, Stejskal J, Sedenkova I, Trchova M, Sapurina I, Cieslar M, Prokes J (2006) Polyaniline nanotubes: conditions of formation. Polym Int 55:31–39. doi:10.1002/pi.1899
19. Liu A, Bac LH, Kim JS, Kim BK, Kim JC (2013) Synthesis and characterization of conducting polyaniline-copper composites. J Nanosci Nanotechnol 13:7728–7733. doi:10.1166/jnn.2013.7831
20. Sapurina IY and Shishov MA Oxidative polymerization of aniline: molecular synthesis of polyaniline and the formation of supramolecular structures. Edited by Ailton De Souza Gomes. http://www.intechopen.com/books/new-polymers-forspecial-applications/oxidative-polymerization-of-aniline-molecular-synthesis-of-polyaniline-and-the-formation-of-supramol. Accessed 12 Sept 2012
21. Chakraborty M, Mandal BM, Mukherjee DC (2005) Oxidative degradation of polyaniline during the chemical oxidative polymerization of aniline in aqueous methanol medium. Polym Int 54:1158–1162. doi:10.1002/pi.1821
22. Dhyani H, Dhand C, Malhotra BD, Sen P (2011) Polyaniline-CdS quantum dots composite for mediator free biosensing. J Biosens Bioelectron 3(112):1–9. doi:10.4172/2155-6210.1000112
23. Pruneanu S, Veress E, Marian I, Oniciu L (1999) Characterization of polyaniline by cyclic voltammetry and UV–Vis absorption spectroscopy. J Mater Sci 34:2733–2739. doi:10.1023/A:1004641908718
24. Snauwaert P, Lazzaroni R, Riga J, Verbist JJ, Gonbeau D (1990) A photoelectron spectroscopic study of the electrochemical processes in polyaniline. J Chem Phys 92:2187–2193. doi:10.1063/1.458010
25. Zhang L, Peng H, Zujovic ZD, Kilmartin PA, Travas-Sejdic J (2007) Characterization of polyaniline nanotubes formed in the presence of amino acids. Macromol Chem Phys 208:1210–1217. doi:10.1002/macp.200700013
26. Chen CF, Lei IA, Chiu WY (2012) Mixed-surfactant-induced morphology change of polyaniline. J Appl Polym Sci 126:E195–E205. doi:10.1002/app.36393